Citation: Molecular Therapy—Nucleic Acids (2016) 5, e296; doi:10.1038/mtna.2016.12
Official journal of the American Society of Gene & Cell Therapy

www.nature.com/mtna

Combination of microRNA-21 and microRNA-146a Attenuates Cardiac Dysfunction and Apoptosis During Acute Myocardial Infarction in Mice

Wei Huang[1], Shan-Shan Tian[1], Peng-Zhou Hang[1], Chuan Sun[1], Jing Guo[1] and Zhi-Min Du[1,2]

Recent studies have revealed the cytoprotective roles of microRNAs (miRNAs) miR-21 and miR-146a against ischemic cardiac injuries. While these studies investigated each of these miRNAs as an independent individual factor, our previous study has suggested the possible interaction between these two miRNAs. The present study was designed to investigate this possibility by evaluating the effects of miR-21 and miR-146a combination on cardiac ischemic injuries and the underlying mechanisms. MiR-21 and miR-146a synergistically decreased apoptosis under ischemia/hypoxic conditions in cardiomyocytes compared with either miR-21 or miR-146a alone. Mice coinjected with agomiR-21 and agomiR-146a had decreased infarct size, increased ejection fraction (EF), and fractional shortening (FS). These effects were greater than those induced by either of the two agomiRs. Furthermore, greater decreases in p38 mitogen-associated protein kinase phosphorylation (p-p38 MAPK) were observed with miR-21: miR-146a combination as compared to application of either of the miRNAs. These data suggest that combination of miR-21 and miR-146a has a greater protective effect against cardiac ischemia/hypoxia-induced apoptosis as compared to these miRNAs applied individually. This synergistic action is mediated by enhanced potency of inhibition of cardiomyocyte apoptosis by the miR-21—PTEN/AKT—p-p38—caspase-3 and miR-146a—TRAF6—p-p38—caspase-3 signal pathways.

Molecular Therapy—Nucleic Acids (2016) **5**, e296; doi:10.1038/mtna.2016.12; published online 15 March 2016
Subject Category: shRNAs, siRAs and MiRNAs; Therapeutic proof of concept

Introduction

Acute myocardial infarction (AMI) is a leading cause of death worldwide and it is characterized by inflammation, cardiomyocyte apoptosis, and cardiac fibrosis and can lead to left ventricular dilatation and heart failure.[1,2] Experimental and clinical studies have shown that cardiomyocyte apoptosis following AMI is caused by oxidative stress, ischemia, and hypoxic injury and reperfusion;[3] mitigating this process is a feasible way of preventing and treating AMI.[4] However, the mechanisms underlying ischemia-induced apoptosis in cardiomyocytes are poorly understood.

MicroRNAs (miRNAs) play a critical role in the pathogenesis of cardiovascular diseases and ischemia-induced apoptosis.[5,6] MiR-21 was shown to prevent myocardial apoptosis against ischemia/reperfusion (I/R)- and H_2O_2-induced cardiomyocyte injury via regulating its target genes programmed cell death 4 (PDCD4) and activator protein 1 (AP1) pathway,[7,8] and reduced cell apoptosis and myocardial infarct size at an early stage of AMI.[9] On the other hand, miR-21 expression is induced by AKT and it in turn produces an antiapoptotic effect by suppressing FasL and activating AKT through inhibiting PTEN, constituting a feed forward loop.[10] Furthermore, miR-21 inhibition decreases p38 MAPK levels in A-498 cells.[11] Moreover, Wang *et al.*[12] identified the protective effect of miR-146a against myocardial I/R injury which can attenuate activation of nuclear factor κB (NF-κB) by repressing expression of interleukin-1 receptor-associated kinase1 (IRAK1) and tumor necrosis factor (TNF) receptor-associated factor 6 (TRAF6). In addition, a recent study showed that miR-146a together with IRAK1, TRAF6 and p-p38 constitutes a negative feed-forward loop that can disrupt cytokine protein synthesis in human THP-1 monocytes.[13,14]

MiRNAs regulate the expression of multiple genes by binding to target transcripts through imperfect sequence complementarity. While the modulation of a single target by an individual miRNA may sometime have only subtle effects, simultaneous repression of multiple genes can have significant impacts on cells.[15] This has been confirmed for miR-21 and its target genes PDCD4, PTEN, sprouty 1 (SPRY1), and SPRY2, as well as for miR-146a and its targets TRAF6 and IRAK1 in cardiovascular disease.[12,16] The capacity of miRNAs to target multiple genes makes them useful therapeutic tools that can be more potent than agents that act on a single gene. Moreover, recent studies from our group[17]and others[15,18–20] have revealed a new mechanism of miRNA action whereby miRNA pairs act synergistically on target genes, leading to a potentiation of their biological effects. Synergistic interactions can increase the efficacy of therapeutics while reducing their side effects and slowing the development of drug resistance. In a previous study, we developed a topological parameter synergy score to evaluate the global synergistic miRNA regulation of apoptosis under pathophysiological conditions and identified a number of antiapoptotic miRNA pairs, including

The first two authors contributed equally to this work.

[1]Institute of Clinical Pharmacology of the Second Affiliated Hospital, Harbin Medical University, Harbin, China; [2]The University Key Laboratory of Drug Research, Heilongjiang Province, Harbin, China. Correspondence: Zhi-Min Du, Institute of Clinical Pharmacology of the Second Affiliated Hospital, Harbin Medical University, Xuefu Road 246#, Nangang District, Harbin 150086, China. E-mail: dzm1956@126.com

Keywords: apoptosis; myocardial infarction; miR-21; miR-146a
Received 13 January 2016; accepted 28 January 2016; published online 15 March 2016. doi:10.1038/mtna.2016.12

the miR-21: miR-146a pair.[17] We conjectured that combined treatment with miR-21 and miR-146a would protect cardiomyocytes against cell death induced by ischemia to a greater extent than either of these two miRNAs. To test this hypothesis, we compared the antiapoptotic effects of miR-21 or miR-146a alone and in combination of the two in cultured neonatal cardiomyocytes and a mouse model of AMI.

Results

Cytoprotective effect of miR-21: miR-146a miRNA pair against hypoxia-induced cardiomyocyte apoptosis

We evaluated the effects of cotransfected miR-146a and miR-21 on hypoxia-induced cellular injury in primary neonatal rat cardiomyocytes. MiR-146a and miR-21 levels were increased when transfected with either one or both miRNAs (**Figure 1a**,**b**). To determine whether cotransfection produces a synergistic effect on cell viability, dose–response curves and combination indices were calculated from cell viability data obtained from cardiomyocytes cultured under hypoxic conditions. The lowest combination index was 0.43 when cell viability was 0.72, indicating a synergistic effect (**Figure 1c**). Under these conditions, the concentration of miR-21 and miR-146a was 40 + 40 nmol/l for a total concentration of 80 nmol/l. We compared the viability of cardiomyocytes transfected with different miR-21/miR-146a ratios (40/40, 20/60, or 60/20 nmol/l) under hypoxia. Cell viability was reduced under hypoxic conditions; cotransfection of miR-21 and miR-146a abrogated this reduction (**Figure 1d**). A ratio of 40/40 nmol/l had a more pronounced effect in terms of restoring cell viability than ratios of 60/20 or 20/60. Therefore, a 40/40 nmol/l combination was used for subsequent experiments. The hypoxia-induced decrease in cell viability was partially restored by treatment with miR-21 or miR-146 alone or in combination (**Figure 1e**). Notably, cotransfection of miR-21 and miR-146a produced the greatest effect than either miR-21 or miR-146a alone ($P < 0.01$), which was reversed by application of miR-21 and miR-146a inhibitors (**Figure 1e**).

In order to determine whether the decrease in cell viability induced by hypoxia could be ascribed to apoptotic cell death and the rescuing effect of miR-21: miR-146a pair could be explained by their potential antiapoptotic action, we first used TUNEL assay to detect DNA fragmentation for apoptosis. We found that hypoxia increased TUNEL-positive cells indicating apoptosis as compared to normoxic conditions (32.9 ± 1.8 versus 6.7 ± 0.7%; $P < 0.01$) (**Figure 2a**,**b**). The number of apoptotic cells was markedly decreased in the presence of miR-21 or miR-146a, and this decrease was more pronounced with the presence of both miRNAs. These effects were all reversed by inhibitor treatment (**Figure 2a**,**b**).

Next, we measured the changes of expression and activities of caspase-3, a known key downstream protease that executes the apoptotic cascade.[21,22] As illustrated in **Figure 2c**,**d**, hypoxia increased the level of caspase-3 mRNA and activity as compared to normoxic controls. These pro-apoptotic changes were blocked by transfection of miR-21 and miR-146a either individually or in combination; a greater effect was observed in the latter instance.

Cytoprotective effect of miR-21: miR-146a miRNA pair against ischemia-induced cardiomyocyte apoptosis

We then tried to clarify whether the antiapoptotic effects of miR-21 and miR-146a seen in cultured cells under hypoxia conditions also exist under in vivo conditions in AMI. **Figure 3a**,**b** shows that AMI significantly increased cardiomyocyte apoptosis, and treatment with miR-21 and miR-146a, whether in combination or individually, drastically decreased this ischemic apoptosis compared with the sham-treated mice. Moreover, in accordance with our *in vitro* experiments under hypoxic conditions, the miR-21: miR-146a pair also produced a remarkably greater magnitude of alleviation of apoptosis than treatment with the individual miRNAs.

Furthermore, ischemia increased caspase-3 mRNA levels by ~5.5 fold (**Figure 3c**) and activity by ~3.0 fold (**Figure 3d**), compared with the sham control. As expected, the miR-21: miR-146a pair produced greater effects on ischemia-induced activation of caspase-3 than miR-21 or miR-146a alone.

MiR-21: miR-146a miRNA pair decreases infarct size and improves cardiac function

Real-time PCR performed 24 hours after injection confirmed the successful delivery of miR-21 and miR-146a into the myocardium as evidenced by 4.9- and 5.3-fold increases in miR-21 and miR-146a levels, respectively (**Figure 4a**,**b**). We found that AMI increased serum lactate dehydrogenase (LDH) activity (a marker for cardiac injury) by 3.0-fold compared to the control group, which was significantly attenuated by agomiR-21/agomiR-146a. No significant difference in LDH activity was observed between agomiR-21 and agomiR-146a being injected in combination or individually (**Figure 4c**).

We next detected the functional role of agomiR-21/agomiR-146a in infarct heart, and found that agomiR-21/agomiR-146a significantly reduced the infarct size in MI (**Figure 4d**,**e**). Moreover, echocardiographic data indicated that ejection fraction (EF) and fractional shortening (FS) were significantly reduced in AMI, but agomiR-21/agomiR-146a increased these parameters indicating improved cardiac function by these miRNAs (**Figure 4g**,**h**). The protective effects of miR-21/miR-146a cotransfection were efficiently blocked by antagomiR-21/antagomiR-146a. No significant difference in intraventricular septum thickness in diastole, intraventricular septum thickness in systole (IVSS), left ventricle posterior wall diameter in end-diastole, and left ventricle posterior wall diameter in end-systole were observed between agomiR-21 and agomiR-146a being injected in combination or individually (**Supplementary Table S1**). Notably, in agreement with our *in vitro* results, miR-21/miR-146a combinational treatment produced a significantly greater protective effect on the ischemic myocardium than single-miRNA treatment.

MiR-21: miR-146a miRNA pair produces beneficial effects by increasing AKT activity and decreasing p38 activity

PTEN and TRAF6 are the direct targets of miR-21 and miR-146a, respectively.[12,16] We therefore examined these two proteins in ischemic hearts. As depicted in **Figure 5a**,**b**, miR-21 or miR-146a alone downregulated the protein levels of PTEN and TRAF6, respectively, in ischemic hearts and a similar effect was observed with the miR-21: miR-146a pair.

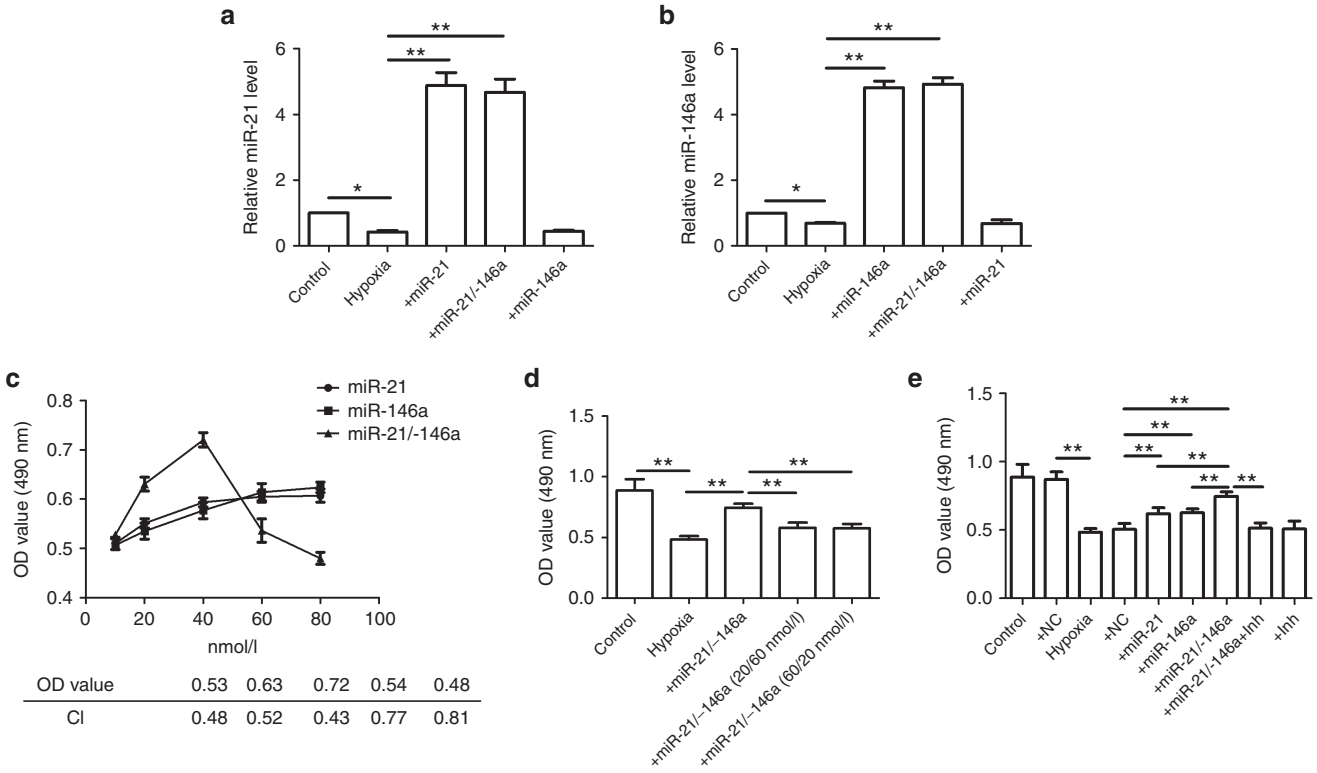

Figure 1 Prosurviving effects of miR-21: miR-146a miRNA pair against hypoxia-induced cardiomyocyte death in cultured neonatal rat ventricular myocytes (NRVMs). Cells were transfected with miR-mimics for 36 hours, and then treated with hypoxia for 12 hours. (**a**,**b**) Changes of expression of miR-21 and miR-146a determined by real-time PCR. $n = 4$/group. (**c**) Dose–response curves (miR-21 or miR-146a: 10, 20, 40, 60, and 80 nmol/l; miR-21/-146a: 10/10, 20/20, 40/40, 60/60, 80/80 nmol/l). $n = 6$/group. (**d**) Cell viability in the ratios of miR-21/-146a under hypoxia. $n = 6$/group. (**e**) Cell viability determined by MTT assay. $n = 6$/group. Data are shown as mean ± standard error of the mean, $^{**}P < 0.01$, one-way analysis of variance.

MiR-21 has been shown to participate in ischemic postconditioning-mediated cardiac protection against I/R injury and cardiac dysfunction through the PTEN/AKT signaling pathway.[23] To see if the same pathway was also involved in our model, we determined the expression of the phosphorylated or activated form of AKT (p-AKT), which directly reflects the activity of the AKT signaling pathway. Ischemia did not affect the level of total AKT (**Figure 5c**); however, this caused a significant decrease (62.5%) in p-AKT compared to the sham group (**Figure 5c**). Coinjection of agomiR-21 and agomiR-146a or agomiR-21 alone either significantly increased the p-AKT in ischemic cardiomyocytes (**Figure 5c**).

P38 MAPK is known to transduce apoptotic or death signal in cardiomyocytes, and enhanced activation (or phosphorylation) of p38 MAPK contributes to myocardial apoptosis.[24] We thus investigated whether agomiR-21/agomiR-146a affect p38 MAPK activities (p-p38) in our model. Three days post-MI, ischemia did not affect the expression level of total p38 MAPK (**Figure 5d**), but caused a significant increase in p38 MAPK phosphorylation with a 2.3-fold increase of p-p38 MAPK expression compared with the sham group (**Figure 5d**). Furthermore, coinjection of agomiR-21 and agomiR-146a significantly inhibited the activation of p38 MAPK in ischemic myocardium to a greater extent than agomiR-21 or agomiR-146a alone (**Figure 5d**).

We used siRNA to silence TRAF6 and PTEN expression and then determined p-p38 MAPK protein expression. The efficiency of TRAF6 and PTEN knock-down by the siRNAs was verified at both mRNA and protein levels, which were otherwise significantly decreased in cardiomyocytes relative to siRNA-NC (**Figure 6a**–**c**,**e**). Next, we examined total p-38 and p-p38 MAPK expression in cells transfected with TRAF6 and PTEN siRNAs. Our results showed that TRAF6 or PTEN siRNA did not affect the expression of total p38 MAPK (lower panel, **Figure 6c**,**f**), but caused a significant decrease in p38 MAPK phosphorylation compared with the control group (upper panel, **Figure 6c**,**f**). Our western blot data showed that the ratio of p-AKT to total AKT increased in PTEN knock-down cardiomyocytes (**Figure 6g**), consistent with the view that PTEN is a negative regulator of AKT, which can cause cell death.[25] To validate that miR-21—PTEN/p-AKT regulates p-p38, expression of p-AKT and p-p38 was detected in cells treated with miR-21 mimic or PI3K inhibitor LY294002 (**Figure 6h**,**i**). MiR-21 significantly abolished hypoxia-induced inactivation of AKT and activation of p38, and these effects were reversed by LY294002 (**Figure 6h**,**i**). Inhibition of p38 MAPK by SD203580 decreased hypoxia-induced apoptosis and caspase-3 activity (**Supplementary Figure S1**). In conclusion, miR-21/miR-146a synergistically inhibited p-p38/caspase-3 against myocardial apoptosis (**Figure 6J**).

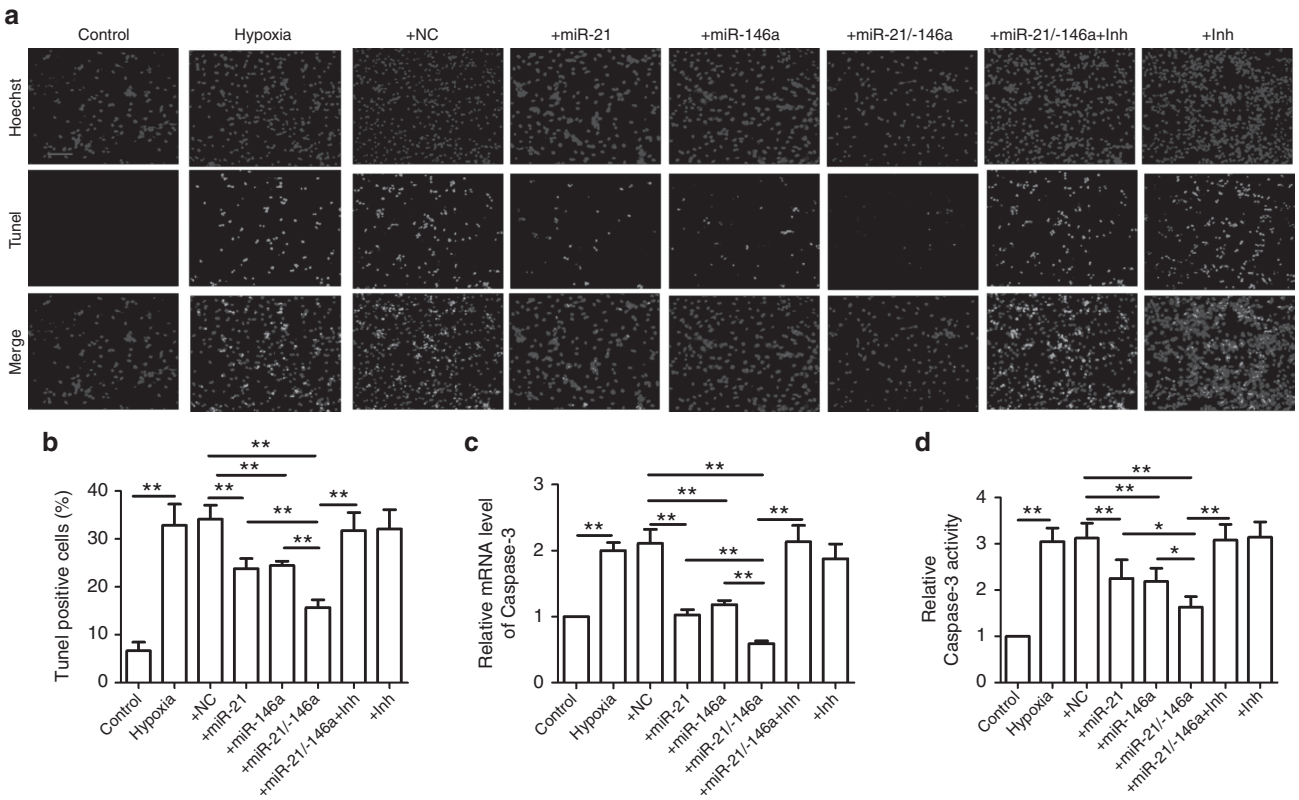

Figure 2 Anti-apoptotic effect of miR-21: miR-146a miRNA pair against hypoxia-induced cardiomyocyte apoptosis in NRVMs. (**a**) Effects of miR-21/miR-146a on cardiomyocytes apoptosis assessed by TUNEL staining. Scale bar = 100 μm. (**b**) TUNEL-positive cell (%). *n* = 6/group. (**c**) Caspase-3 mRNA level determined by real-time PCR. *n* = 4/group. (**d**) Caspase-3 activity determined by colorimetric assay. *n* = 6/group. Data are shown as means ± standard error of the mean, $^{*}P < 0.05$, $^{**}P < 0.01$, one-way analysis of variance.

Discussion

It has been well accepted that miRNAs play important roles in regulating every aspects of myocardial injuries and cardiac function in the setting acute myocardial infarction. While the published studies primarily focus on the role of individual miRNAs, the possibly interactions between miRNAs remained scarcely investigated despite that such interactions are being increasingly recognized. It is clear that multiple miRNAs coexist in the cardiac cells and their actions are not isolated from one another if miRNA-miRNA interactions are in place. The present study shed light on this issue. The main findings of this study include: (i) miR-21/miR-146a synergistically reduced ischemia/hypoxia-induced cardiomyocyte apoptosis both *in vivo* and *in vitro*; (ii) miR-21/miR-146a synergistically reduced infarct size and ameliorated the impaired cardiac function of infarct mice *in vivo*; and (iii) miR-21/miR-146a synergistically inhibits cardiomyocyte apoptosis through the miR-21—PTEN/AKT—p-p38—caspase-3 and miR-146a—TRAF6—p-p38—caspase-3 signaling pathways. The synergistic actions confer an enhanced cytoprotective power afforded by the miRNAs against ischemic apoptotic cell death leading to ameliorated myocardial injuries and improved cardiac function in infarct hearts. Our study thus unraveled a novel mode of miRNA actions at the layer of two-miRNA combination that offers synergistic regulation on basic cell biology process and the associated conditions such as ischemic cardiac disease.

Recent studies found two miRNAs combination synergistically therapy of some diseases. MiR-34 and let-7 combination synergistically suppressed non-small-cell lung cancer growth.[15] MiRNA-143 and miRNA-145 synergistically inhibit the growth of human bladder cancer cells.[18] Coinhibition of miRNA-10b and miRNA-21 exerts synergistic inhibition on the proliferation and invasion of human glioma cells.[19] However, miRNA combination was seldom investigated in heart disease, for instance combination of miRNA-499 and miRNA-133 exerts a synergic effect on cardiac differentiation.[20] MiRNAs are known to play important roles in the pathological conditions involving apoptosis, including AMI and heart failure.[26] Among these apoptosis-regulating miRNAs, miR-21 and miR-146a have both been documented to elicit antiapoptotic effects thereby beneficial effects on ischemic myocardial injury;[7–10,12] however, whether there exists a synergistic action between these two miRNAs similar to those reported for two miRNAs combination was unknown. Here, we used an *in vitro* hypoxia model and *in vivo* ischemic model to demonstrate the antiapoptotic effects and the cellular signaling mechanisms of the miR-21: miR-146a pair. Our results showed that ischemia/hypoxia induced significant myocardial injury, as reflected by increased cardiomyocyte apoptosis, increased infarct size, elevated LDH activity, and decreased EF and FS. All these anomalies were alleviated

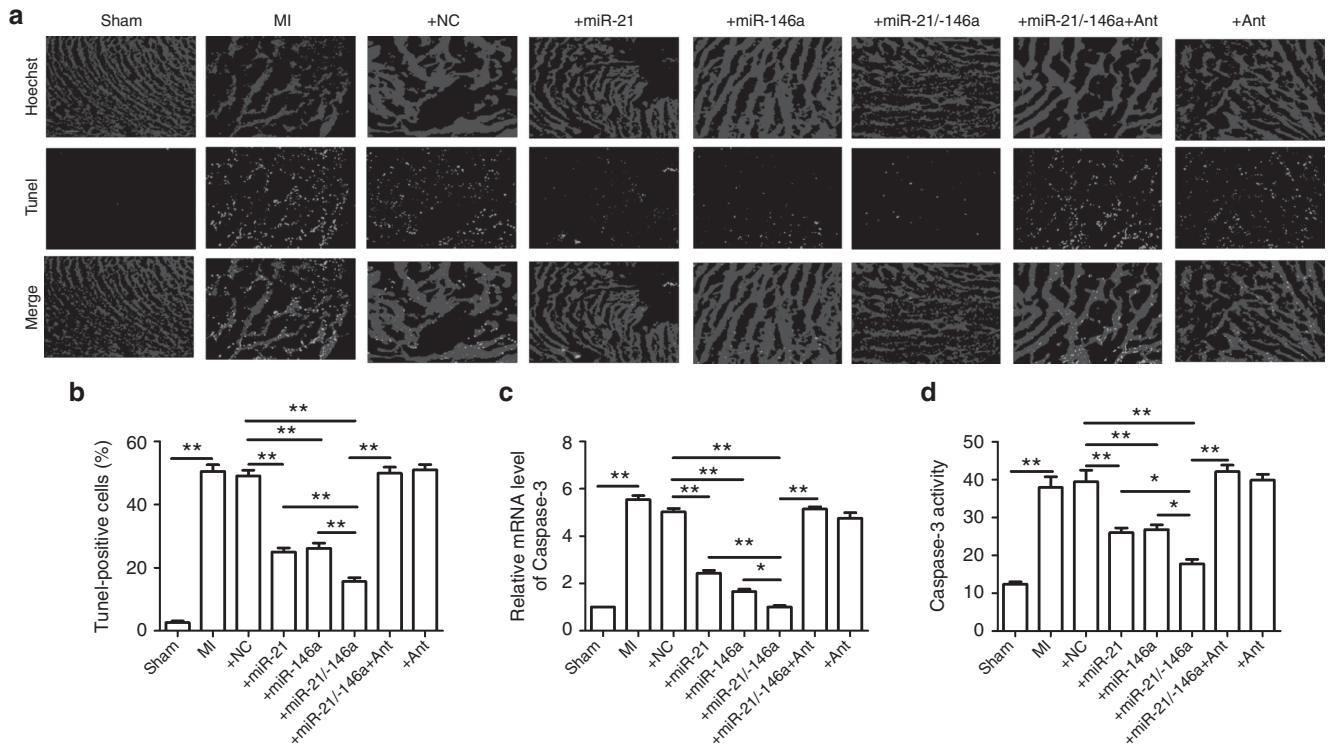

Figure 3 Cytoprotective effect of the miR-21: miR-146a miRNA pair against ischemia-induced cardiomyocyte apoptosis in a mouse model of acute myocardial infarction (AMI). (**a**) Effects of miR-21/miR-146a on cardiac apoptosis evaluated by TUNEL staining. Scale bar = 100 μm. (**b**) TUNEL-positive cell (%). $n = 8$/group. (**c**) Caspase-3 mRNA level determined by real-time PCR. $n = 4$/group. (**d**) Caspase-3 activity determined by colorimetric assay. $n = 8$/group ($^*P < 0.05$, $^{**}P < 0.01$, one-way analysis of variance).

by miR-21/miR-146a combination treatment, confirming the cardio-protective property of these miRNAs. Moreover, miR-21/miR-146a combination produced greater benefit effects than each of these miRNAs separately.

We have also identified the signaling pathway responsible for the antiapoptotic effects of miR-21/miR-146a against ischemia-/hypoxia-induced myocardial injuries. In this study, we observed an activation of caspase-3, as the key protease executing the apoptotic cascade in the intrinsic and extrinsic apoptotic pathways,[27–29] in cardiomyocytes during ischemia and hypoxia. MiR-21 and miR-146a reversed the ischemia-/hypoxia-induced abnormal enhancement of caspase-3 activity. Notably, the combination of the two miRNAs consistently produced stronger effects than each miRNA individually.

Many reports have demonstrated that p38 MAPK plays an important role in ischemia-induced apoptosis with its activation by phosphorylation contributing to cardiac injury,[24,30] and treatment with a pharmacological inhibitor of p38 MAPK SB203580 can prevent cardiomyocyte death.[31,32] Recent studies found miR-146a by directly targeting IRAK1 and TRAF6 limits p38 MAPK activation.[13,14,33,34] Whether miR-146a mediated TRAF6-p-p38 MAPK signaling pathway contributes to ischemia/hypoxia-induced apoptosis in cardiomyocytes has not been previously studied. In agreement with previous studies, we found that miR-146a downregulated TRAF6 in ischemic cardiomyocytes accounting partially for the antiapoptotic efficacy of this miRNA, consistent with our observation that direct silencing of TRAF6 by siRNA decreased the level of p-p38 MAPK in neonatal rat cardiomyocytes.

Overexpression of miR-21 in a transgenic mouse model resulted in suppression of ischemia-induced upregulation of PTEN expression,[35] increase in p-AKT expression, reduction of infarct size, and amelioration of heart failure. PTEN is a major negative regulator of AKT[36] whose activity is modulated by its abundance, oxidation, or phosphorylation.[37] Regulation of the p38 pathway by AKT and the impact on cell survival have been reported in several other models, including endothelial cells[38] and β-cell,[39] and in E1A-induced apoptosis.[40] Whether miR-21 elicited PTEN/AKT-p-p38 MAPK signaling contributes to ischemia-/hypoxia-induced apoptosis in cardiomyocytes has not been previously studied. As further evidence, we showed that miR-21 suppressed PTEN and upregulated p-AKT in ischemic cardiomyocytes. Moreover, PTEN siRNA decreased the level of p-p38 MAPK but increased p-AKT in neonatal rat cardiomyocytes. Furthermore, PI3K inhibitor LY294002 increased the level of p-p38 MAPK and decreased p-AKT in hypoxia-induced neonatal rat cardiomyocytes. Additionally, inhibiting p38 MAPK attenuated the hypoxia-induced increases in cardiomyocytes apoptosis and caspase-3 activity. On the basis of these findings, we proposed that suppression of the p38 MAPK/caspase-3 cascade may be an underlying mechanism of miR-21 and miR-146a against ischemic injury in AMI hearts. It should be noted that inhibition of the p38 MAPK/caspase-3 signal pathway may merely be one of the protective mechanisms of miR-21/ miR-146a combination in ischemic cardiomyocytes. While other signaling pathways may also contribute to the antiapoptotic property

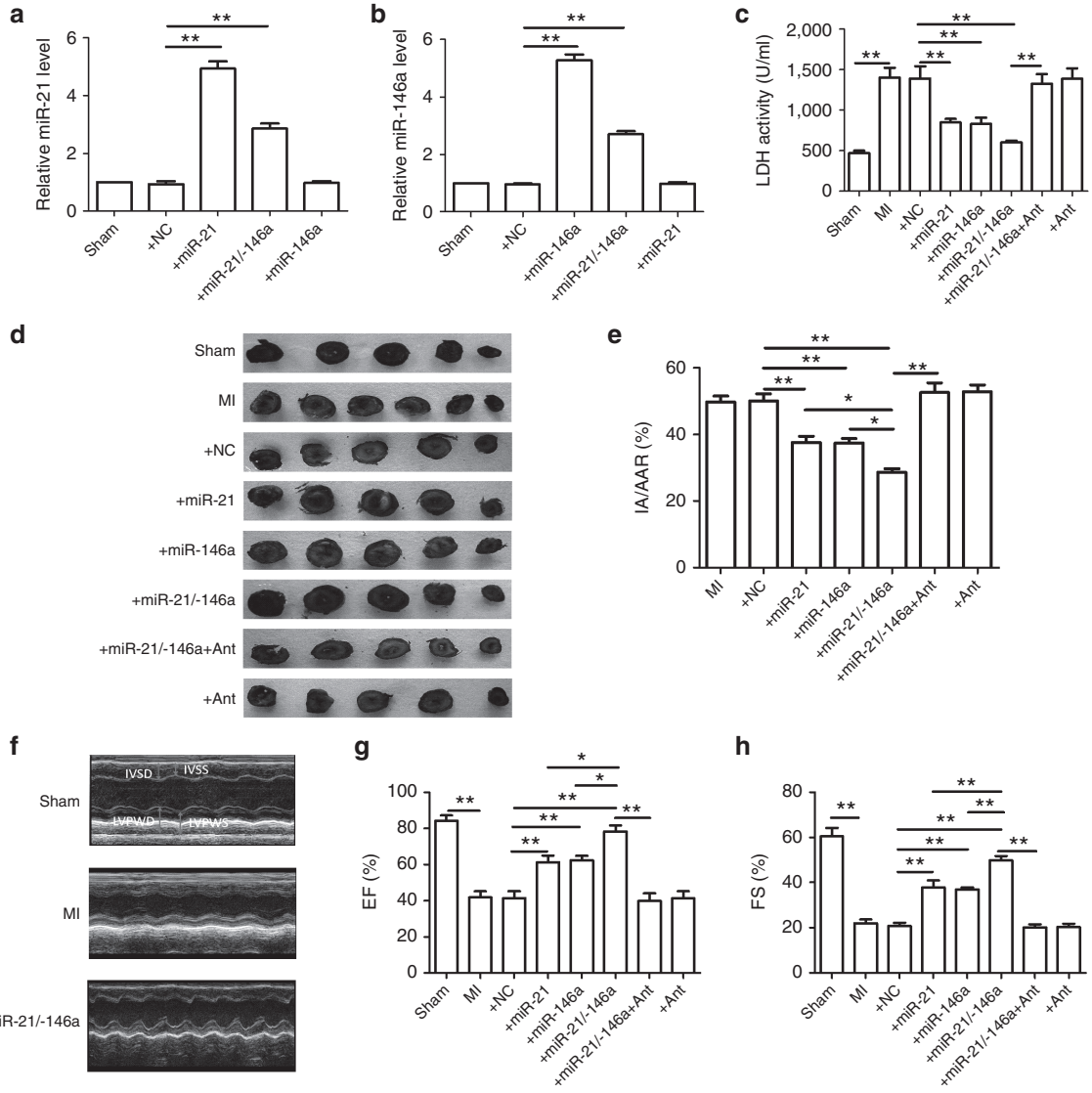

Figure 4 Reduction of infarct size and improvement of cardiac function by the miR-21: miR-146a pair in AMI mice. (**a,b**) Transcript levels of miR-21 and miR-146a determined by real-time PCR. *n* = 4/group. (**c**) Serum lactate dehydrogenase activity in MI and agomiR-21/agomiR-146a mice. *n* = 8/group. (**d**) Representative images showing infarct areas in cross section slices. (**e**) Statistical analysis of IA/AAR ratio. AAR, area at risk; IA, infarct area. *n* = 8/group. (**f**) Representative photographs of heart function. IVSD, intraventricular septum thickness in diastole; IVSS, intraventricular septum thickness in systole; LVPWD, left ventricle posterior wall diameter in end-diastole; LVPWS, left ventricle posterior wall diameter in end-systole. (**g**) Ejection fractions. *n* = 8/group. (**h**) Fractional shortening. *n* = 8/group (**P* < 0.05, ***P* < 0.01, one-way analysis of variance).

of these miRNAs, our results do not in any way exclude this possibility.

As a whole, our study revealed that the combination of miR-21 and miR-146a offers a superior effect against cardiac ischemia-/hypoxia-induced apoptosis compared with either miR-21 or miR-146a alone. The synergistic action may be mediated by the miR-21—PTEN/AKT—p-p38—caspase-3 and miR-146a—TRAF6—p-p38—caspase-3 signaling pathways. Our study implies that miR-21/miR-146a combination may be a new therapeutic candidate in the treatment of ischemic heart diseases.

Materials and methods

Animals. Healthy adult male Kunming mice (25–30 g) were used in this study. Mice were maintained with food and water under standard animal room conditions (temperature 23 ± 1 °C; humidity 55 ± 5%). All experimental protocols were in accordance with and approved by the Experimental Animal Ethic Committee of Harbin Medical University, China. Use of animals complied with the Guide for the Care and Use of Laboratory Animals published by the US National Institutes of Health (NIH Publication, 8th Edition, 2011).

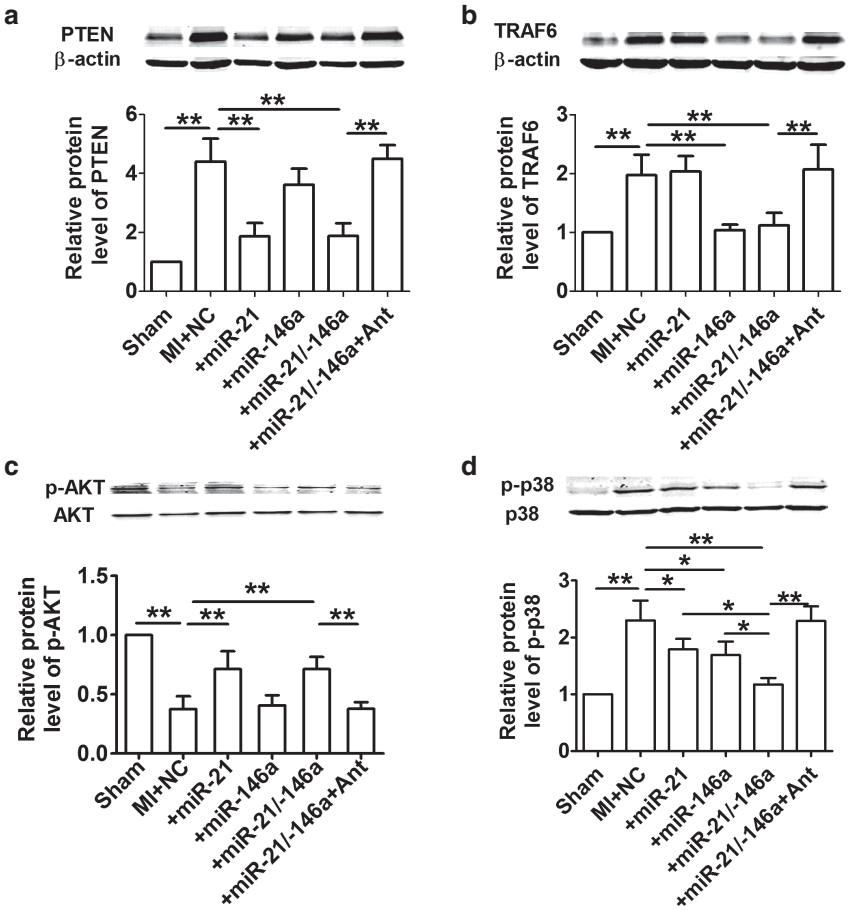

Figure 5 Changes of protein levels of PTEN, TRAF6, p-AKT, and p-p38 in AMI mice. (**a**) Representative western blot bands of PTEN protein. $n = 5$/group. (**b**) Representative western blot bands of TRAF6 protein. $n = 4$/group. (**c**) Representative western blot bands of p-AKT and AKT proteins. $n = 4$/group. (**d**) Representative western blot bands of p-p38 and p38 proteins. Values given were normalized to the band intensity of β-actin as an internal control. $n = 4$/group ($^{*}P < 0.05$, $^{**}P < 0.01$, one-way analysis of variance).

Administration of agomiR-21/-miR-146a and their antagomiRs. The agomiR-21 and agomiR-146a (Ribo-bio, Guangzhou, China) are double-stranded RNA analogues identical to the mature mmu-miR-21-5p (5′-UAGCUUAUCAG ACUGAUGUUGA-3′) and mmu-miR-146a-5p (5′-UGAGAAC UGAAUUCCAUGGGUU-3′). MiRNA negative control (miR-NC) sequence is (5′-UUUGUACUACACAAAAGUACUG-3′). All these constructs were chemically modified and conjugated with cholesterol moiety for *in vivo* applications with long-lasting stability and enhanced target specificity and affinity. The mice were randomly divided into the following groups: Sham, MI, MI + NC, agomiR-21 (100 nmol·kg^{-1}), agomiR-146a (100 nmol·kg^{-1}), agomiR-21/miR-146a (50/50 nmol·kg^{-1}), antagomiR-21/miR-146a (100/100 nmol·kg^{-1}), agomiR-21/miR-146a (50/50 nmol·kg^{-1}), and antagomiR-21/miR-146a (100/100 nmol·kg^{-1}). AgomiR-21 and agomiR-146a were administered by intramuscular injection into the left ventricle myocardium at multiple sites at a dosage of 100 nmol·kg^{-1} in 0.2 ml saline 24 hours prior to MI.[41] The dosage of agomiR was determined according to the published studies.[41,42] For Sham mice, an equal volume of saline was given.

Mouse model of MI and measurement of infarct size. Mice were subjected to left anterior descending (LAD) coronary artery ligation to induce MI as described previously.[43] Remote tissues of ischemic areas in the left ventricles were quickly dissected for subsequent analysis. The measurement of area at risk and infarct size was according to previous study.[43] Three days after MI, 0.3 ml Evans blue dye (2%, Sigma Aldrich St. Louis, MO) was injected retrogradely into the vena cava to delineate the region of myocardial perfusion. After washing out remaining blood and trimming out the right ventricle, the left ventricle was cut into 2-mm thick slices and stained with 1% triphenyltetrazolium chloride at 37 °C for 10 minutes, and the infarct area was stainless while the live area turned red. The area at risk (ischemic area) and infarct area were calculated using Image ProPlus 5.0 software (Media Cybernetics, Wokingham, UK). For further study, the tissues in ischemic area of the hearts were collected and stored at –80 °C.

Echocardiographic measurements. Three days post-MI, the changes in left ventricular function were evaluated by transthoracic echocardiography with an ultrasound machine (Panoview β1500, Cold Spring Biotech, Taiwan, China) equipped with a 30-MHz phased-array transducer. Left ventricular EF and FS were calculated from M-mode recording. Meanwhile, intraventricular septum thickness in diastole, intraventricular septum thickness in systole, left ventricle

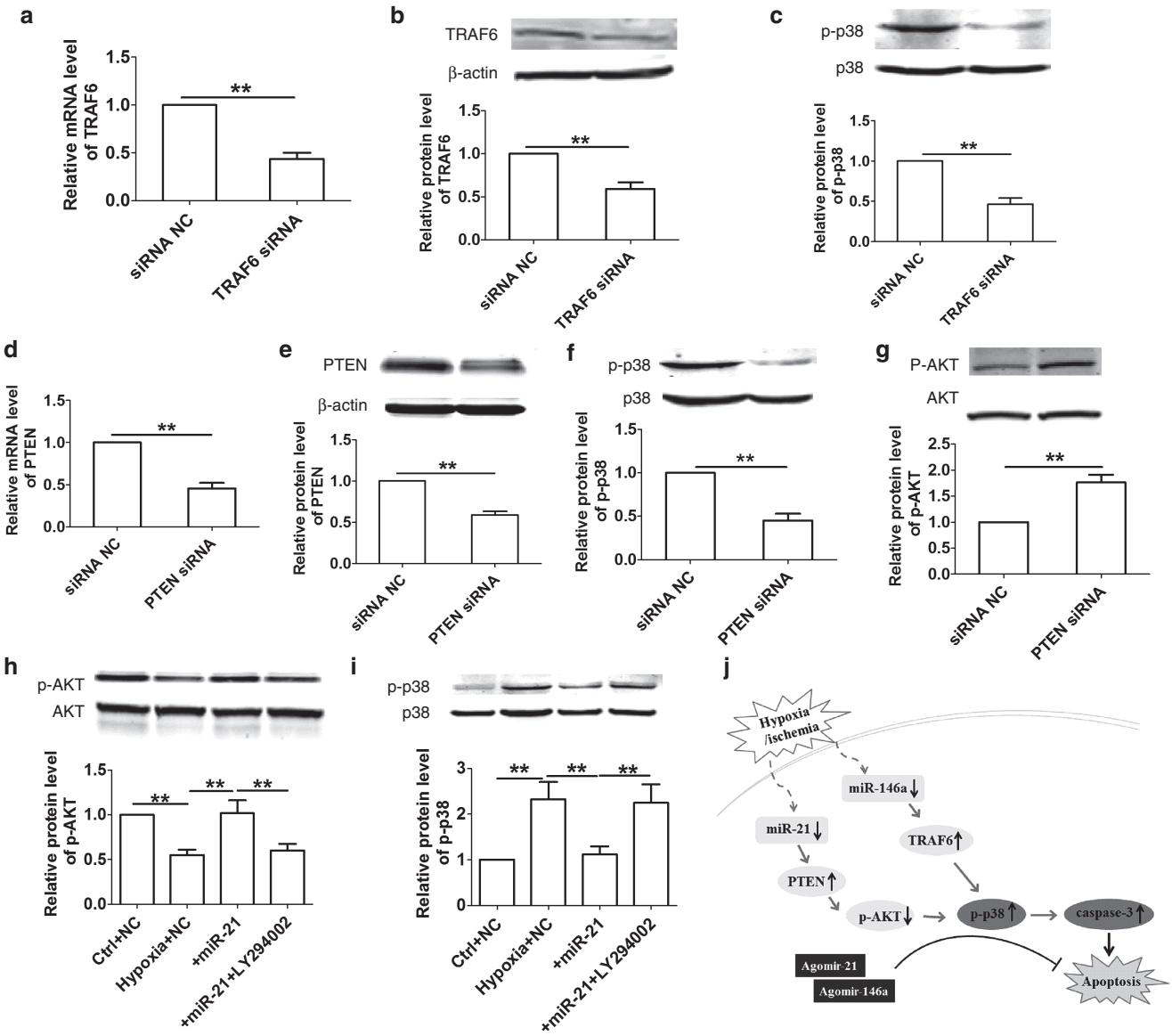

Figure 6 Synergistic suppression of p-p38 MAPK by the miR-21: miR-146a pair in neonatal rat ventricular myocytes. (**a,b**) Verification of the efficacy and specificity of TRAF6 siRNA in silencing TRAF6 at both mRNA and protein levels. *n* = 4/group. (**c**) Effect of TRAF6 siRNA on the protein level of p-p38. *n* = 4/group. (**d,e**) Verification of the efficacy and specificity of PTEN siRNA in silencing PTEN at both mRNA and protein levels. *n* = 4/group. (**f,g**) Changes of p-p38 and p-AKT levels in PTEN siRNA transfected cells. *n* = 4/group. (**h,i**) Effects of PI3K inhibitor LY294002 on p-AKT and p-p38 levels. Cells were preincubated with LY294002 (10 μmol/l) for 2 hours, then transfected with miR-21 for 36 hours, and finally treated with hypoxia for 12 hours. *n* = 4/group (*$P < 0.05$, **$P < 0.01$, one-way analysis of variance). (**j**) The diagram illustrating the synergistic mechanism of miR-21: miR-146a pair attenuates apoptosis.

posterior wall diameter in end-diastole, and left ventricle posterior wall diameter in end-systole were measured.

Neonatal rat ventricular myocytes culture and transfection. The procedures to culture neonatal rat ventricular myocytes were the same as described previously.[44] Briefly, the hearts of neonatal Wistar rats were rapidly removed, minced in serum-free Dulbecco's Modified Eagle Media (DMEM, HyClone, Logan, UT), and then digested in 0.25% trypsin solution. Dispersed cells were suspended in Dulbecco's Modified Eagle Media (DMEM, HyClone) containing 10% fetal bovine serum and centrifuged. The isolated cells were plated into culture flasks (noncoated) and 0.1 mmol/l bromodeoxyuridine was added into the medium to deplete nonmyocytes. Cardiomyocytes were cultured under a condition of 5% CO_2 at 37 °C.

MiR-21-mimic, miR-146a-mimic, miR-21 inhibitor, miR-146a inhibitor, and NC were synthesized by Guangzhou RiboBio (Guangzhou, China). PTEN siRNA and TRAF6 siRNA were purchased from Santa Cruz Biotechnology (Santa Cruz, CA). Cardiomyocytes (1×10^5 per well) were starved in serum-free medium for 24 hours before transfection with X-treme GENE siRNA transfection reagent (Roche, Penzberg Germany) according to the manufacturer's instructions. The dosage of miR-mimic was determined based

upon our previous study.[17] Thirty-six hours after transfection, neonatal rat ventricular myocytes were treated with hypoxia under 1% O_2, 5% CO_2, and 94% N_2 for 12 hours in a modular incubator. Caspase-3-specific inhibitor z-DEVD-fmk (20 μmol/l) was purchased from Merck, Darmstadt, Germany. PI3K inhibitor LY294002 (10 μmol/l) and p38MAPK inhibitor SB203580 (20 μmol/l) were purchased from Sigma.

Quantitative real-time reverse transcription-PCR. Total RNA from cultured neonatal cardiomyocytes after different treatments or heart tissue was extracted using TRIZOL reagent (Invitrogen, Carlsbad, CA) according to the manufacturer's protocols. The levels of caspase-3, PTEN, TRAF6, miR-21, and miR-146a mRNA were determined using SYBR Green incorporation on Roche LightCycler480 Real Time PCR system (Roche, Germany), with U6 as an internal control for miR-21 and miR-146a and GAPDH for caspase-3, PTEN, and TRAF6. The sequences of primers were: miR-21 forward: 5′-GGGGTAGCTTATCAG ATCG-3′ and reverse: 5′-TGGAGTCGGCAATTGCACTG-3′; miR-146a forward: 5′-GGGTGAGAACTGAATTCCAT-3′ and reverse: 5′-TCGGCAATTGCACTGGATAC-3′; U6 forward:5′-GCTTCGGCACATATACTAAAAT-3′ and reverse: 5′-CGCTTC ACGAATTTGCGTGTCAT-3′; GAPDH forward: 5′-AAGAAGGT GGTGAAGCAGGC-3′ and reverse: 5′-TCCACCACCCAGTT GCTGTA-3′; PTEN forward: 5′-TGGATTCGACTTAGACTTGA CCT-3′ and reverse: 5′-GCGGTGTCATAATGTCTCTCAG-3′; TRAF6 forward: 5′-AAAGCGAGAGATTCTTTCCCTG-3′ and reverse: 5′-ACTGGGGACAATTCACTAGAGC-3′ and caspase-3 forward: 5′-CTCGCTCTGGTACGGATGTG-3′ and reverse: 5′-TCCCATAAATGACCCCTTCATCA-3′. The amount of target ($2^{-\Delta\Delta^{CT}}$) was obtained by normalizing to endogenous reference and relative to a calibrator (average of the control samples).

Serum LDH assay. The blood samples were collected from mice 72 hours after occlusion of the coronary artery and the activity of myocardial specific enzyme LDH was measured with the colorimetric method according to the manufacture's protocols (Nanjing Jiancheng Bioengineering Institute, Nanjing, China).

Caspase-3 activity assay. Myocardial caspase-3 activity was determined by use of colorimetric assay kits (Beyotime Institute of Biotechnology, Jiangsu, China) according to the manufacturer's instructions. After experimental treatments, cardiomyocytes were centrifuged (600 ×g, 4 °C, 5 minutes) and washed with ice-cold PBS. Cells were then lysed in ice-cold cell lysis buffer for 15 minutes. Samples were centrifuged at 20,000 ×g for 10 minutes at 4 °C, and 30 μl supernatant samples were incubated with 10 μl of substrate (2 mmol/l Ac-DEVD-pNA) in 60 μl of assay buffer at 37 °C for 2 hours. The absorbance was measured at 405 nm.

Terminal deoxynucleotidyl transferase dUTP nick end labeling (TUNEL). Apoptosis of cardiomyocyte was detected by staining ventricular specimens and neonatal rat ventricular myocytes with the *In situ* Cell Death Detection Kit (TUNEL fluorescence FITC kit, Roche) according to the manufacturer's instruction. After TUNEL staining, the ventricular specimens (3 days post-MI) or cardiomyocytes (12 hours after hypoxia) were immerged into the Hoechst 33342 (Sigma-Aldrich) solution to stain nuclei of living and apoptotic cells. Fluorescence staining was viewed under a laser scanning confocal microscope (Olympus, Fluoview1000, Tokyo, Japan). Numbers of apoptotic cardiomyocytes are presented as the percentage of total cells counted.

MTT assay and combination index calculation. Cells (2×10^4 cells/well) were seeded in a 96-well culture plate. Cell viability was measured by 3-(4,5-dimethylthiazol-2-yl)-2,5-diphenyltetrazolium bromide (MTT) assay according to the manufacturer's instructions. The absorbance was measured at 490 nm. The combination index value was calculated by using the Calcusyn software (Biosoft, Cambridge, UK) based on the median effect equation as previously reported in details.[45] A combination index value < 1, =1, or >1 denotes synergism, additive effect, or antagonism, respectively.

Western blot analysis. Total protein samples were extracted from peri-infarct region of left ventricular myocardium for immunoblotting analysis.[41] Protein sample (70 μg) was fractionated by SDS-PAGE (10 % polyacrylamide gels) and transferred to nitrocellulose membrane. The membranes were blocked in 5% nonfat milk PBS for 2 hours and then incubated at 4 °C overnight with the following primary antibodies: p38 MAPK (Cell Signaling Technology, Danvers, MA), p-p38MAPK (Cell Signaling Technology, Danvers, MA), TRAF6 (Santa Cruz Biotechnology, Santa Cruz, CA), PTEN (Proteintech Group, Chicago, IL), p-AKT (Cell Signaling Technology, Danvers, MA), AKT (Cell Signaling Technology, Danvers, MA), and β-actin (ZSJZ-Bio, Beijing, China). After washing, the membrane was incubated with secondary antibody for 1 hour. Images were captured on the Odyssey CLx Infrared Imaging System (LI-COR Biosciences, Lincoln, NE). Western blot bands were quantified using Odyssey CLx v2.1 software (LI-COR Biosciences, Lincoln, NE). The data were normalized to β-actin as an internal control.

Data analysis. Group data are expressed as mean ± standard error of the mean. Statistical comparisons between two groups were performed by *t*-test, and among multiple groups were performed by one-way analysis of variance followed by Tukey's multiple comparison tests. Differences were considered to be statistically significant when $P < 0.05$. Data were analyzed using the GraphPad Prism 5.0 (GraphPad Software, La Jolla, CA) and SPSS 14.0 (SPSS, Chicago, IL).

Supplementary material

Table S1. Ventricular thickness (mm) obtained from the echocardiographic analysis of the mice three days after AMI.
Figure S1. Inhibition of p38 MAPK by SD203580 decreased hypoxia-induced apoptosis and caspase-3 activity.

Acknowledgments This work was supported in part by the Major Program of National Natural Science Foundation of China (81230081), Specialized Research Fund for the Doctoral Program of Higher Education of China (20112307130004). All authors declare that they have no competing interests for this study.

1. Wartenberg, KE (2012). Malignant middle cerebral artery infarction. *Curr Opin Crit Care* **18**: 152–163.
2. Bogomolov, AN, Kozlov, KL, Kurochkina, ON and Olesiuk, IB (2013). [Coronary stenting in elderly patients with acute myocardial infarction (review)]. *Adv Gerontol* **26**: 151–160.
3. Chen-Scarabelli, C, Saravolatz, L Jr, Murad, Y, Shieh, WS, Qureshi, W, Di Rezze, J *et al.* (2012). A critical review of the use of carvedilol in ischemic heart disease. *Am J Cardiovasc Drugs* **12**: 391–401.
4. Hojo, Y, Saito, T and Kondo, H (2012). Role of apoptosis in left ventricular remodeling after acute myocardial infarction. *J Cardiol* **60**: 91–92.
5. Ren, XP, Wu, J, Wang, X, Sartor, MA, Qian, J, Jones, K *et al.* (2009). MicroRNA-320 is involved in the regulation of cardiac ischemia/reperfusion injury by targeting heat-shock protein 20. *Circulation* **119**: 2357–2366.
6. Thum, T, Catalucci, D and Bauersachs, J (2008). MicroRNAs: novel regulators in cardiac development and disease. *Cardiovasc Res* **79**: 562–570.
7. Cheng, Y, Zhu, P, Yang, J, Liu, X, Dong, S, Wang, X *et al.* (2010). Ischaemic preconditioning-regulated miR-21 protects heart against ischaemia/reperfusion injury via anti-apoptosis through its target PDCD4. *Cardiovasc Res* **87**: 431–439.
8. Cheng, Y, Liu, X, Zhang, S, Lin, Y, Yang, J and Zhang, C (2009). MicroRNA-21 protects against the H(2)O(2)-induced injury on cardiac myocytes via its target gene PDCD4. *J Mol Cell Cardiol* **47**: 5–14.
9. Dong, S, Cheng, Y, Yang, J, Li, J, Liu, X, Wang, X *et al.* (2009). MicroRNA expression signature and the role of microRNA-21 in the early phase of acute myocardial infarction. *J Biol Chem* **284**: 29514–29525.
10. Sayed, D, He, M, Hong, C, Gao, S, Rane, S, Yang, Z *et al.* (2010). MicroRNA-21 is a downstream effector of AKT that mediates its antiapoptotic effects via suppression of Fas ligand. *J Biol Chem* **285**: 20281–20290.
11. Zaman, MS, Shahryari, V, Deng, G, Thamminana, S, Saini, S, Majid, S *et al.* (2012). Up-regulation of microRNA-21 correlates with lower kidney cancer survival. *PLoS One* **7**: e31060.
12. Wang, X, Ha, T, Liu, L, Zou, J, Zhang, X, Kalbfleisch, J *et al.* (2013). Increased expression of microRNA-146a decreases myocardial ischaemia/reperfusion injury. *Cardiovasc Res* **97**: 432–442.
13. Brudecki, L, Ferguson, DA, McCall, CE and El Gazzar, M (2013). MicroRNA-146a and RBM4 form a negative feed-forward loop that disrupts cytokine mRNA translation following TLR4 responses in human THP-1 monocytes. *Immunol Cell Biol* **91**: 532–540.
14. Brudecki, L, Ferguson, DA, McCall, CE and El Gazzar, M (2013). Mitogen-activated protein kinase phosphatase 1 disrupts proinflammatory protein synthesis in endotoxin-adapted monocytes. *Clin Vaccine Immunol* **20**: 1396–1404.
15. Kasinski, AL, Kelnar, K, Stahlhut, C, Orellana, E, Zhao, J, Shimer, E *et al.* (2015). A combinatorial microRNA therapeutics approach to suppressing non-small cell lung cancer. *Oncogene* **34**: 3547–3555.
16. Cheng, Y and Zhang, C (2010). MicroRNA-21 in cardiovascular disease. *J Cardiovasc Transl Res* **3**: 251–255.
17. Zhu, W, Zhao, Y, Xu, Y, Sun, Y, Wang, Z, Yuan, W *et al.* (2013). Dissection of protein interactomics highlights microRNA synergy. *PLoS One* **8**: e63342.
18. Noguchi, S, Yasui, Y, Iwasaki, J, Kumazaki, M, Yamada, N, Naito, S *et al.* (2013). Replacement treatment with microRNA-143 and -145 induces synergistic inhibition of the growth of human bladder cancer cells by regulating PI3K/Akt and MAPK signaling pathways. *Cancer Lett* **328**: 353–361.
19. Dong, CG, Wu, WK, Feng, SY, Wang, XJ, Shao, JF and Qiao, J (2012). Co-inhibition of microRNA-10b and microRNA-21 exerts synergistic inhibition on the proliferation and invasion of human glioma cells. *Int J Oncol* **41**: 1005–1012.
20. Pisano, F, Altomare, C, Cervio, E, Barile, L, Rocchetti, M, Ciuffreda, MC *et al.* (2015). Combination of miRNA499 and miRNA133 exerts a synergic effect on cardiac differentiation. *Stem Cells* **33**: 1187–1199.
21. Porter, AG and Jänicke, RU (1999). Emerging roles of caspase-3 in apoptosis. *Cell Death Differ* **6**: 99–104.
22. Saikumar, P, Dong, Z, Mikhailov, V, Denton, M, Weinberg, JM and Venkatachalam, MA (1999). Apoptosis: definition, mechanisms, and relevance to disease. *Am J Med* **107**: 489–506.
23. Tu, Y, Wan, L, Fan, Y, Wang, K, Bu, L, Huang, T *et al.* (2013). Ischemic postconditioning-mediated miRNA-21 protects against cardiac ischemia/reperfusion injury via PTEN/Akt pathway. *PLoS One* **8**: e75872.
24. Szokodi, I, Kerkelä, R, Kubin, AM, Sármán, B, Pikkarainen, S, Kónyi, A *et al.* (2008). Functionally opposing roles of extracellular signal-regulated kinase ½ and p38 mitogen-activated protein kinase in the regulation of cardiac contractility. *Circulation* **118**: 1651–1658.
25. Hers, I, Vincent, EE and Tavaré, JM (2011). Akt signalling in health and disease. *Cell Signal* **23**: 1515–1527.
26. Li, P (2010). MicroRNAs in cardiac apoptosis. *J Cardiovasc Transl Res* **3**: 219–224.
27. Fernandes-Alnemri, T, Litwack, G and Alnemri, ES (1994). CPP32, a novel human apoptotic protein with homology to Caenorhabditis elegans cell death protein Ced-3 and mammalian interleukin-1 beta-converting enzyme. *J Biol Chem* **269**: 30761–30764.
28. Salvesen, GS (2002). Caspases: opening the boxes and interpreting the arrows. *Cell Death Differ* **9**: 3–5.
29. Yang, B, Ye, D and Wang, Y (2013). Caspase-3 as a therapeutic target for heart failure. *Expert Opin Ther Targets* **17**: 255–263.
30. Marber, MS, Rose, B and Wang, Y (2011). The p38 mitogen-activated protein kinase pathway–a potential target for intervention in infarction, hypertrophy, and heart failure. *J Mol Cell Cardiol* **51**: 485–490.
31. Ma, XL, Kumar, S, Gao, F, Louden, CS, Lopez, BL, Christopher, TA *et al.* (1999). Inhibition of p38 mitogen-activated protein kinase decreases cardiomyocyte apoptosis and improves cardiac function after myocardial ischemia and reperfusion. *Circulation* **99**: 1685–1691.
32. Liu, Y, Zhang, S, Su, D, Liu, J, Cheng, Y, Zou, L *et al.* (2015). Inhibiting (pro)renin receptor-mediated p38 MAPK signaling decreases hypoxia/reoxygenation-induced apoptosis in H9c2 cells. *Mol Cell Biochem* **403**: 267–276.
33. Nahid, MA, Pauley, KM, Satoh, M and Chan, EK (2009). miR-146a is critical for endotoxin-induced tolerance: implication in innate immunity. *J Biol Chem* **284**: 34590–34599.
34. Taganov, KD, Boldin, MP, Chang, KJ and Baltimore, D (2006). NF-kappaB-dependent induction of microRNA miR-146, an inhibitor targeted to signaling proteins of innate immune responses. *Proc Natl Acad Sci USA* **103**: 12481–12486.
35. Roy, S, Khanna, S, Hussain, SR, Biswas, S, Azad, A, Rink, C *et al.* (2009). MicroRNA expression in response to murine myocardial infarction: miR-21 regulates fibroblast metalloprotease-2 via phosphatase and tensin homologue. *Cardiovasc Res* **82**: 21–29.
36. Hlobilková, A, Knillová, J, Bártek, J, Lukás, J and Kolár, Z (2003). The mechanism of action of the tumour suppressor gene PTEN. *Biomed Pap Med Fac Univ Palacky Olomouc Czech Repub* **147**: 19–25.
37. Leslie, NR, Batty, IH, Maccario, H, Davidson, L and Downes, CP (2008). Understanding PTEN regulation: PIP2, polarity and protein stability. *Oncogene* **27**: 5464–5476.
38. Gratton, JP, Morales-Ruiz, M, Kureishi, Y, Fulton, D, Walsh, K and Sessa, WC (2001). Akt down-regulation of p38 signaling provides a novel mechanism of vascular endothelial growth factor-mediated cytoprotection in endothelial cells. *J Biol Chem* **276**: 30359–30365.
39. Widenmaier, SB, Ao, Z, Kim, SJ, Warnock, G and McIntosh, CH (2009). Suppression of p38 MAPK and JNK via Akt-mediated inhibition of apoptosis signal-regulating kinase 1 constitutes a core component of the beta-cell pro-survival effects of glucose-dependent insulinotropic polypeptide. *J Biol Chem* **284**: 30372–30382.
40. Liao, Y and Hung, MC (2003). Regulation of the activity of p38 mitogen-activated protein kinase by Akt in cancer and adenoviral protein E1A-mediated sensitization to apoptosis. *Mol Cell Biol* **23**: 6836–6848.
41. Yang, B, Lin, H, Xiao, J, Lu, Y, Luo, X, Li, B *et al.* (2007). The muscle-specific microRNA miR-1 regulates cardiac arrhythmogenic potential by targeting GJA1 and KCNJ2. *Nat Med* **13**: 486–491.
42. Lu, Y, Zhang, Y, Wang, N, Pan, Z, Gao, X, Zhang, F *et al.* (2010). MicroRNA-328 contributes to adverse electrical remodeling in atrial fibrillation. *Circulation* **122**: 2378–2387.
43. Pan, Z, Sun, X, Ren, J, Li, X, Gao, X, Lu, C *et al.* (2012). miR-1 exacerbates cardiac ischemia-reperfusion injury in mouse models. *PLoS One* **7**: e50515.
44. Ai, J, Zhang, R, Gao, X, Niu, HF, Wang, N, Xu, Y *et al.* (2012). Overexpression of microRNA-1 impairs cardiac contractile function by damaging sarcomere assembly. *Cardiovasc Res* **95**: 385–393.
45. Chou, TC (2010). Drug combination studies and their synergy quantification using the Chou-Talalay method. *Cancer Res* **70**: 440–446.

Supplementary Information accompanies this paper on the Molecular Therapy–Nucleic Acids website (http://www.nature.com/mtna)